

# Wettability and interfacial energies in SiC–liquid metal systems

P. NIKOLOPOULOS, S. AGATHOPOULOS, G. N. ANGELOPOULOS

Laboratory of Physical Metallurgy, Department of Chemical Engineering, University of Patras, 26110 Patras, Greece

A. NAOUMIDIS, H. GRÜBMEIER

Institute for Reactor Materials, KFA—Research Centre, Jülich, P.O. Box 1913, D-5170 Jülich, Germany

The sessile drop technique is used to measure the contact angles of molten Si, Sn, Cu and Ni in contact with mono- and polycrystalline  $\alpha$ -SiC as well as CVD  $\beta$ -SiC in purified argon atmosphere and at various temperatures. The contact angle of silicon, near its melting point, is about  $38^\circ$  on a mono- as well as polycrystalline  $\alpha$ -SiC substrate and about  $41.5^\circ$  on  $\beta$ -SiC. Tin does not wet the SiC. Using data from the available literature, the work of adhesion and the interfacial energy between SiC and Si or Sn were calculated. In the  $\alpha$ -SiC–Sn system, both quantities are linearly dependent on temperature in the investigated temperature range 523–1073 K. The metals copper and nickel react with silicon carbide. The silicon content of the copper drop depends on the annealing temperature. The nickel drop after cooling forms the compound  $\text{Ni}_3\text{Si}_2$ . The interferometric measured groove angle of SiC (thermal etching) in vacuum at 2020 K gives a mean value of  $157.6 \pm 5.8^\circ$ .

## 1. Introduction

Modern engineering ceramics possess significant advantages over metallic materials for a variety of technical applications. Existing disadvantages, such as brittleness and insufficient reproducibility of properties, are being addressed by current research projects. Furthermore, suitable techniques for joining ceramic materials with each other and with metals are being developed [1]. With regard to the commercial viability of engineering ceramics, techniques are required for the joining of ceramics to metallic components [2]. Brazing, diffusion welding and those processes in which one of the work pieces involved is fused are suitable for application in the high-temperature range which is of particular interest.

For high-temperature structural applications, silicon carbide-based ceramics are currently being considered due to their good mechanical strength and oxidation resistance at elevated temperatures.

Generally, the wettability conditions between ceramics and liquid-metal phases are of importance in the development of joining techniques. The correlation between the wetting and the bonding behaviour at the interface in solid–liquid–vapour systems in thermodynamic equilibrium is given by the equation

$$W_\alpha = \gamma_{SV} + \gamma_{LV} - \gamma_{SL} \quad (1)$$

where  $\gamma_{SV}$ ,  $\gamma_{LV}$  are the surface energies of the solid and liquid phases, respectively,  $\gamma_{SL}$  is the interfacial energy of solid–liquid, and  $W_\alpha$  the work of adhesion, defined as the work needed to separate an interface [3]. An established method for studying the interfacial phe-

nomena is that of a sessile drop of liquid metal lying on a ceramic substrate (Fig. 1). In this case the following equation holds

$$\gamma_{SV} = \gamma_{SL} + \gamma_{LV} \cos \theta \quad (2)$$

where  $\theta$  is the contact angle. Introducing Equation 2 into Equation 1 we obtain

$$W_\alpha = \gamma_{LV}(1 + \cos \theta) \quad (3)$$

The ratio of the grain-boundary energy,  $\gamma_{SS}$ , to the surface energy,  $\gamma_{SV}$ , of polycrystalline ceramics is given by the equation

$$\gamma_{SS}/\gamma_{SV} = 2 \cos \psi/2 \quad (4)$$

where  $\psi$  is the equilibrium angle that develops at the surface (Fig. 2).

This work therefore makes a contribution to the development of joining techniques by investigating the wettability properties of SiC in contact with molten Si and various metals such as Sn, Cu and Ni.

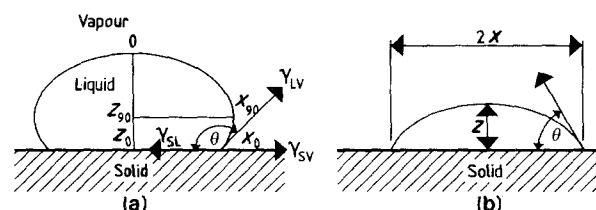


Figure 1 Contact angle  $\theta$  in the solid–liquid–vapour system in equilibrium.

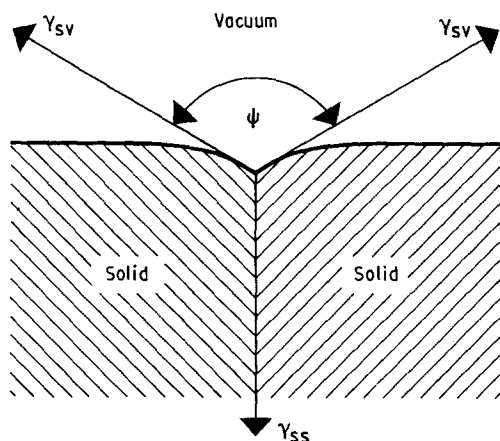


Figure 2 Groove angle  $\psi$  in the polycrystalline solid-vapour system.

## 2. Experimental procedure

The materials used for the wetting measurements were silicon carbides with a metallographic polished surface. The following qualities were used:

- (a) High-dense sintered  $\alpha$ -SiC (ESK Kempton);
- (b)  $\alpha$ -SiC single crystals;
- (c)  $\beta$ -SiC deposited by the CVD method on graphite substrate.

Silicon of the quality specified for the semiconductor industry was used for the sessile drop experiments. The metals used in rod form had a purity better than 99.995% as given by the manufacturer (Ventron GmbH).

Measurements of the contact angle,  $\theta$ , were carried out in a purified argon atmosphere. The samples were heated by an induction furnace. Optical windows permitted photography of the sessile drop as well as measurement of the temperature by optical pyrometry.

Each experiment lasted for about 20–30 min. Photographs of the sessile drop were obtained at 5-min intervals. The influence of metal vapours existing in the furnace atmosphere has proved to be of minor importance for the surface energy of the ceramic and the values of the wetting angles, and has therefore been neglected.

Optical interferometry was used to measure the groove angle  $\psi$ . In order to observe the undisturbed interference pattern, large grains are desirable, and the silicon carbide quality from ESK was not suitable. For this purpose, SiC containing  $B_4C$  additives was sintered at the Josef Stefan Institute, Ljubljana/YU, for 1 h at 2330 K, and post-heated for recrystallization for 1 h at 2470 K. Metallographic polished samples of this material were thermally etched in a vacuum of  $10^{-5}$  mb at 2020 K for 1 and 2 h.

The root angle  $\psi$  can be calculated from the apparent angle  $\alpha$  from the following equation [4]

$$\tan \frac{\psi}{2} = \frac{2d}{1.11 \lambda m} \tan \frac{\alpha}{2} \quad (5)$$

where  $d$  = width between the groove shoulders,  $\lambda$  = wavelength of the light source, and  $m$  = magnification. The factor 1.11 is used to correct the effect of

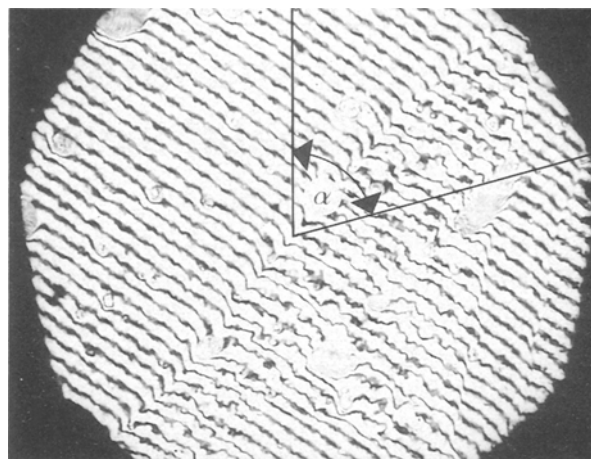


Figure 3 Interference patterns to obtain the groove angle  $\psi$  of  $\alpha$ -SiC ( $T = 2020$  K,  $t = 1$  h,  $\lambda = 589$  nm).

the large aperture of the objective lens. Fig. 3 shows the interference patterns thus obtained.

## 3. Results and discussion

If the contact angle,  $\theta$ , in the system examined is greater than  $90^\circ$ , the sessile drop has the form of an ellipsoid of revolution. From the values of  $X_{90}$ ,  $Z_{90}$ ,  $X_0$ ,  $Z_0$  (Fig. 1a) and by using the tables of Bashfort and Adams [5] the contact angle can be determined.

If  $\theta < 90^\circ$ , we assume that the drop has the form of a spherical segment. In this case the contact angle can be calculated according to the relation

$$\operatorname{tg} \theta/2 = Z/X \quad (6)$$

(Fig. 1b). In the system SiC–Si with different silicon carbide substrates, a good wettability is observed and the contact angle,  $\theta$ , is independent of annealing time (Fig. 4). For mono- as well as polycrystalline  $\alpha$ -SiC, the  $\theta$  values are quite similar, i.e. about  $38^\circ$  at temperatures near the melting point of silicon. This value agrees reasonably well with results reported by Wahlen and Anderson ( $40 \pm 5^\circ$  in vacuum at 1750 K [6]), Naidich *et al.* ( $36^\circ$  in vacuum at 1750 K [7]) and Yupko and Gnesin ( $33$ – $37^\circ$  in vacuum at 1720 K [8]).

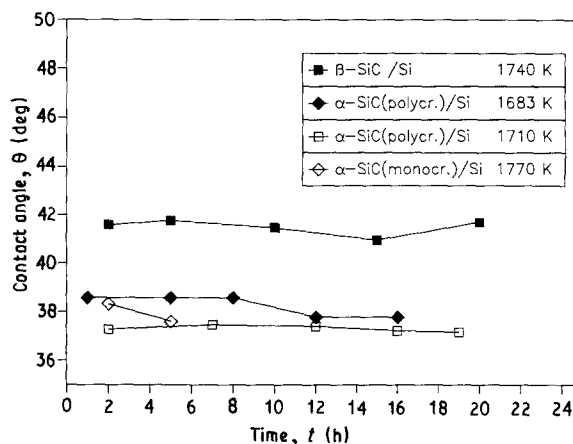


Figure 4 Time dependence of the contact angle  $\theta$  for Si on various SiC substrates.

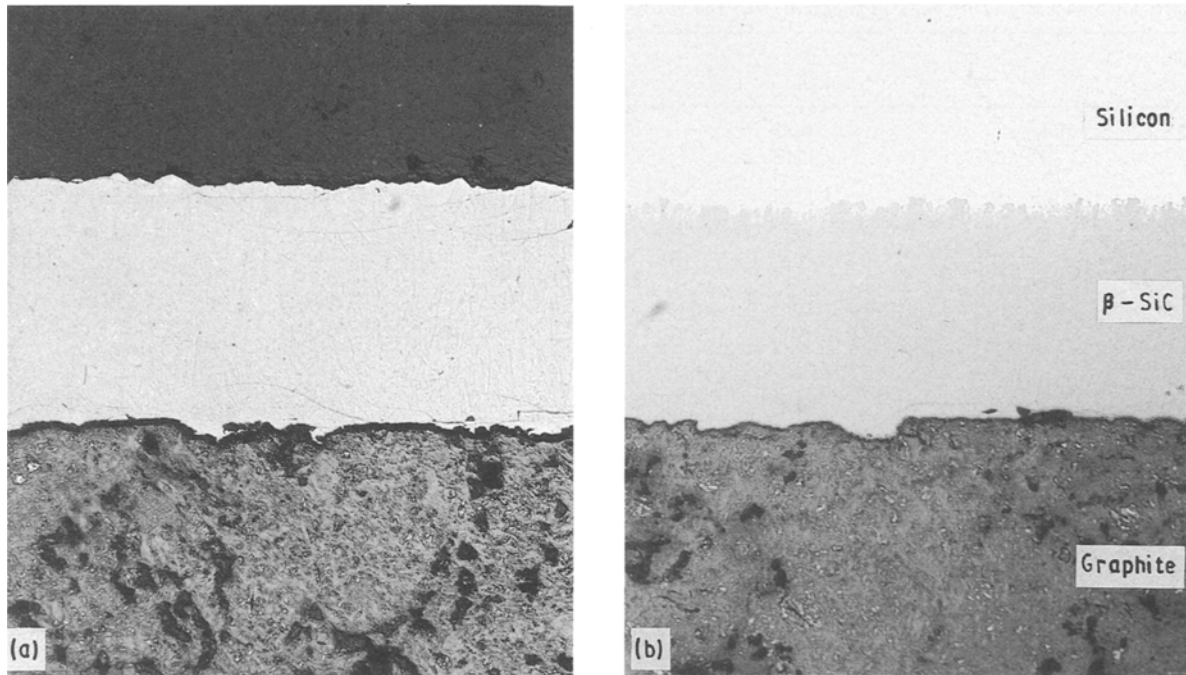


Figure 5 The original surface of  $\beta$ -SiC (a) has been restructured under the influence of molten silicon (b).

A small deviation from this value, i.e.  $41.5^\circ$ , is observed for the  $\beta$ -SiC. This material was used as produced by the CVD process with a roughness  $R_a = 0.5 \mu\text{m}$ , and was not additionally polished. The metallographic cross-section of this sample (Fig. 5) demonstrates surface restructuring of  $\beta$ -SiC, which may be caused by a partial transformation of the metastable  $\beta$ - to thermodynamically stable  $\alpha$ -modification of SiC.

Fig. 6 gives the measured contact angle  $\theta$  of molten Sn ( $T_m = 505 \text{ K}$ ) on a polycrystalline  $\alpha$ -SiC for different temperatures. In this system the contact angle decreases with increasing temperature, but the molten metal does not wet the ceramic in the investigated temperature range. The contact angle did not change with annealing time.

Similar results have already been reported for experiments in a vacuum by Köhler [9] at a temperature range between 850 and 1300 K, and by Naidich and Nevodnik [7] at 1323 K. Also Allen and Kingery [10]

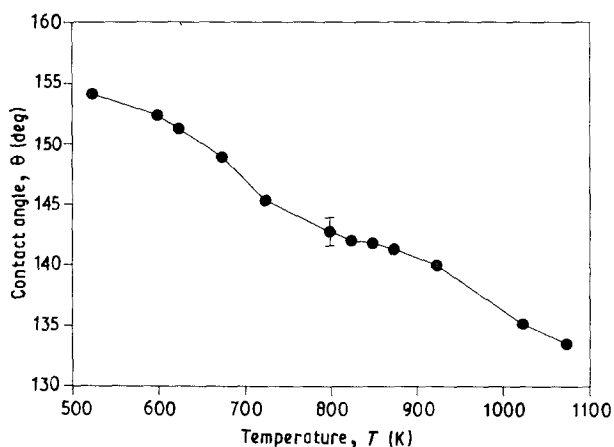
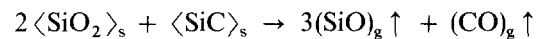


Figure 6 Temperature dependence of contact angle  $\theta$  for Sn on polycrystalline  $\alpha$ -SiC.

measured at 1373 K a contact angle of  $165^\circ$  in the system HP-SiC/Sn, while at a temperature 100 K higher a good wettability ( $\theta = 75^\circ$ ) was observed. This result seems very surprising at first. An explanation for this effect is given in connection with formation of an oxidic thin film ( $\text{SiO}_2$ ) on the SiC surface. Also, in a hydrogen atmosphere this oxidic film seems to be stable because the  $\theta$  value remains at the same high level ( $140^\circ$ ), in good agreement with measurements of the system  $\text{SiO}_2$ -Sn [11]. At temperatures higher than 1475 K in vacuum, this oxidic film disintegrates according to the reaction



Under these conditions a pure SiC surface is formed and the value is therefore more realistic for this system than the measurement at lower temperatures. However, for practical application, i.e. brazing of SiC work pieces, the observed poor wettability with Sn is evident.

The system SiC-Cu has been investigated using polycrystalline  $\alpha$ -SiC as well as CVD- $\beta$ -SiC in a temperature range between 1420 and 1720 K. The observed contact angle did not change within a time of 20 min, but decreased with increasing temperature (see Table I). The angle in this system always remained higher than  $90^\circ$  (Fig. 7) and indicates poor wettability. Microstructural post-examination of those samples shows a reaction zone between Cu and both used SiC qualities (Fig. 8). The thickness of the reaction layers increases with time and with increasing temperature. Measurements with an electron probe microanalyser (EPMA) in the Cu drop indicate an increasing Si content in the Cu melt with the temperature (from  $T = 1580 \text{ K}$  with 1.1 wt % Si, to  $T = 1723 \text{ K}$  with 2.3 wt % Si). According to the Cu-Si phase diagram [12] the Cu drop consists in both cases of the  $\alpha$ -Cu phase.

TABLE I Contact angles ( $\theta$ ), work of adhesion ( $W_\alpha$ ) and interfacial energy ( $\gamma_{SL}$ ) in SiC-liquid-metal systems

System	$T$ (K)	$\theta$ (degrees)	$W_\alpha$ ( $J m^{-2}$ )	$\gamma_{SL}$ ( $J m^{-2}$ )
$\alpha$ -SiC (polycrystalline)/Si	1683	$38.25 \pm 0.44$	1.346	1.489
	1710	$37.27 \pm 0.13$	1.350	1.468
$\alpha$ -SiC (monocrystalline)/Si	1770	$37.96 \pm 0.52$	1.338	1.444
$\beta$ -SiC/Si	1740	$41.49 \pm 0.33$	1.312	1.488
$\alpha$ -SiC(polycrystalline)/Sn	523	$154.11 \pm 1.42$	0.054	3.203
	598	$152.34 \pm 0.51$	0.061	3.149
	623	$151.23 \pm 0.48$	0.066	3.130
	673	$148.86 \pm 0.96$	0.077	3.088
	723	$145.30 \pm 1.20$	0.094	3.040
	798	$142.74 \pm 1.16$	0.107	2.980
	823	$142.01 \pm 0.68$	0.111	2.962
	848	$141.79 \pm 0.52$	0.111	2.946
	873	$141.29 \pm 0.88$	0.114	2.927
	923	$139.98 \pm 0.77$	0.121	2.890
$\alpha$ -SiC(polycrystalline)/Cu	1023	$135.16 \pm 0.49$	0.148	2.801
	1073	$133.51 \pm 0.48$	0.157	2.761
	1423	$133.15 \pm 1.41$	(Reaction)	
	1583	$129.45 \pm 1.10$		
1723	$124.36 \pm 7.77$			
$\beta$ -SiC(polycrystalline)/Cu	1423	$157.09 \pm 3.25$	(Reaction)	
	1573	$142.00 \pm 9.68$		
	1716	$129.70 \pm 6.23$		
$\beta$ -SiC/Ni	1770	74.00	(Reaction)	

The increase of Si content with temperature is a result of the reaction kinetics. An experiment at 1873 K for 4 h resulted in a very large reaction zone, so that the excessive Si concentration in the solidified Cu drop led to a composition between 8.5 and 9.5 wt % Si and 91.5–90 wt % Cu, indicating the formation of silicides. This sample also allowed the examination of the reaction zone by X-ray diffraction (XRD) analysis. We observed the formation of the  $\gamma$  phase ( $Cu_5Si$ ) of the Cu–Si phase diagram (JCPDS 4-0841), but with smaller lattice parameters (Fig. 9).

Gnesin and Naidich [13] reported on similar investigations using monocrystalline  $\alpha$ -SiC as well as self-bonded silicon carbide. According to the soft hardness of the Cu drop, they supposed that after the reaction between  $\alpha$ -SiC and Cu the  $\alpha$ -Cu phase was

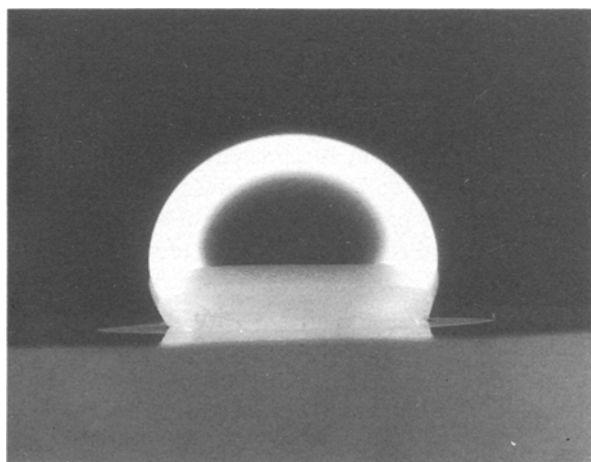


Figure 7 Copper drop on polycrystalline  $\alpha$ -SiC ( $T = 1583$  K,  $t = 20$  min).

also formed. This phase seems to wet the reacted zone of SiC in vacuum, while our results in an argon atmosphere disagree on this point.

Experiments with the SiC–Ni system using polycrystalline  $\alpha$ -SiC and CVD- $\beta$ -SiC at 1770 K result in a strong reaction between the two partners. The measured contact angle for  $\beta$ -SiC–Ni was  $74^\circ$ . Naidich and Nevodnik [7] report an angle of  $65^\circ$  for polycrystalline  $\alpha$ -SiC–Ni. The  $\beta$ -SiC layer with a thickness of  $80 \mu m$  was fully reacted after a heating time of 15 min. The metallographic cross-section of this sample indicates furthermore an interaction with the graphite substrate of the CVD- $\beta$ -SiC layer. In this case, the original Ni drop includes large graphite lamella precipitations formed from the saturated carbon solution in the Ni melt during the cooling process. As a result of this reaction, a wide region of the  $\beta$ -SiC layer outside the contact area with the Ni-melt was transformed in a two-phase product (Fig. 10). Using XRD analysis, graphite was identified as one of these products. Measurements with the electron probe microanalyser identified the second phase as a nickel silicide within the range of  $Ni_{64}Si_{36}$  and  $Ni_{66}Si_{34}$ . Similar results have been obtained in the reaction zone between Ni and  $\alpha$ -SiC. In this case the Ni drop also contains very small graphite precipitations. Quantitative measurements (point analysis) with the EPMA give the following chemical composition in the Ni-drop region:

$$Ni(\text{wt } \%) = 76.4 \pm 0.4$$

$$Si(\text{wt } \%) = 24.8 \pm 0.2$$

This composition corresponds to the phase  $Ni_3Si_2$  which was also found by XRD analysis.

TABLE II Linear temperature functions of surface energies for solid ceramic and liquid metals

Material	Surface energy ( $\text{J m}^{-2}$ )	$T(\text{K})$	Ref.
$\beta$ -SiC (110)	$3.000-0.546 \times 10^{-3} T$ (average)	$0 \leq T$	[16]
Sn	$0.544-0.070 \times 10^{-3} (T - 505)$	$T \geq T_m = 505$	[17]
Si	$0.754-0.070 \times 10^{-3} (T - 1683)$	$T \geq T_m = 1683$	[18]

Thermodynamic estimations made by Klomp [14] for a temperature range of 800–1200 K result in the formation of  $\text{Ni}_3\text{Si}$  after reaction between SiC and Ni. According to the phase diagram for Si–Ni–C pro-

posed by Jackson *et al.* [15] for a temperature of 1150 K, only the  $\text{Ni}_5\text{Si}_3$  ( $\theta$ -phase) is in equilibrium with carbon and SiC. According to the binary phase system reported by Hansen and Anderko [12], this phase is only stable at  $T > 1080$  K. Our results can be considered as a solidified system of a Ni–Si melt containing carbon. It seems that the chemical activity of Ni in this liquid phase has reached an equilibrium composition and does not react with SiC.

The measured contact angles in the SiC–liquid-metal systems, together with data from the literature on the surface energy  $\gamma_{\text{SV}}$  of SiC [16], and of the surface energies  $\gamma_{\text{LV}}$  of the non-reactive liquid metals Sn [17] and Si [18] (Table II) were used for the calculation of the interfacial energy (Equation 2) and the work of adhesion (Equation 3). The results of the measurements of contact angles, as well as the calculated values of the work of adhesion and the interfacial energies in the investigated systems, are given in Table I above. The calculated values for the work of adhesion and the interfacial energy in the system SiC–Si (Table I) agree well with the reported values [19, 20] within this temperature range.

The results show that in the  $\alpha$ -SiC (polycrystalline)–Sn system the work of adhesion and the interfacial energy are linear temperature functions and therefore the following equations are valid:

$$W_{\alpha}(\alpha\text{-SiC}/\text{Sn}) = 0.047 + 0.192 \times 10^{-3} (T - 505) \quad (\text{J m}^{-2}) \quad (7)$$

( $R = 0.9935$ )

$$\gamma_{\text{SL}}(\alpha\text{-SiC})/\text{Sn}) = 3.629 - 0.808 \times 10^{-3} (T - 505) \quad (\text{J m}^{-2}) \quad (8)$$

( $R = 0.9996$ )

where  $R$  is the correlation coefficient. Using Equation 5, the interferometrically measured groove angles (Fig. 3) in a vacuum of  $10^{-5}$  mb at 2020 K of polycrystalline  $\alpha$ -SiC give the mean values

$$\begin{aligned} \psi_{(1)} &= 156.4^\circ \pm 6.8^\circ \text{ at 1 h} \\ \psi_{(2)} &= 158.4^\circ \pm 5.0^\circ \text{ at 2 h} \end{aligned}$$

The number of measured angles are  $n_{(1)} = 34$  and  $n_{(2)} = 58$ . The results reveal that the groove angle  $\psi$  does not vary significantly with annealing time and therefore a mean value of  $\Psi = 157.6 \pm 5.8^\circ$  can be assumed.

Therefore the ratio  $\gamma_{\text{SS}}/\gamma_{\text{SV}}$  (Equation 4) is given as  $0.388 \pm 0.099$ . Using  $\gamma_{\text{SV}} = 1.89 \text{ J m}^{-2}$  at 2020 K (from Table II) the calculated value of the grain-boundary energy of  $\alpha$ -SiC is given as  $\gamma_{\text{SS}} = 0.733 \pm 0.187 \text{ J m}^{-2}$ . This value is about five times smaller than that reported by Minnear [19]:  $\gamma_{\text{SS}} = 3.46 \text{ J m}^{-2}$

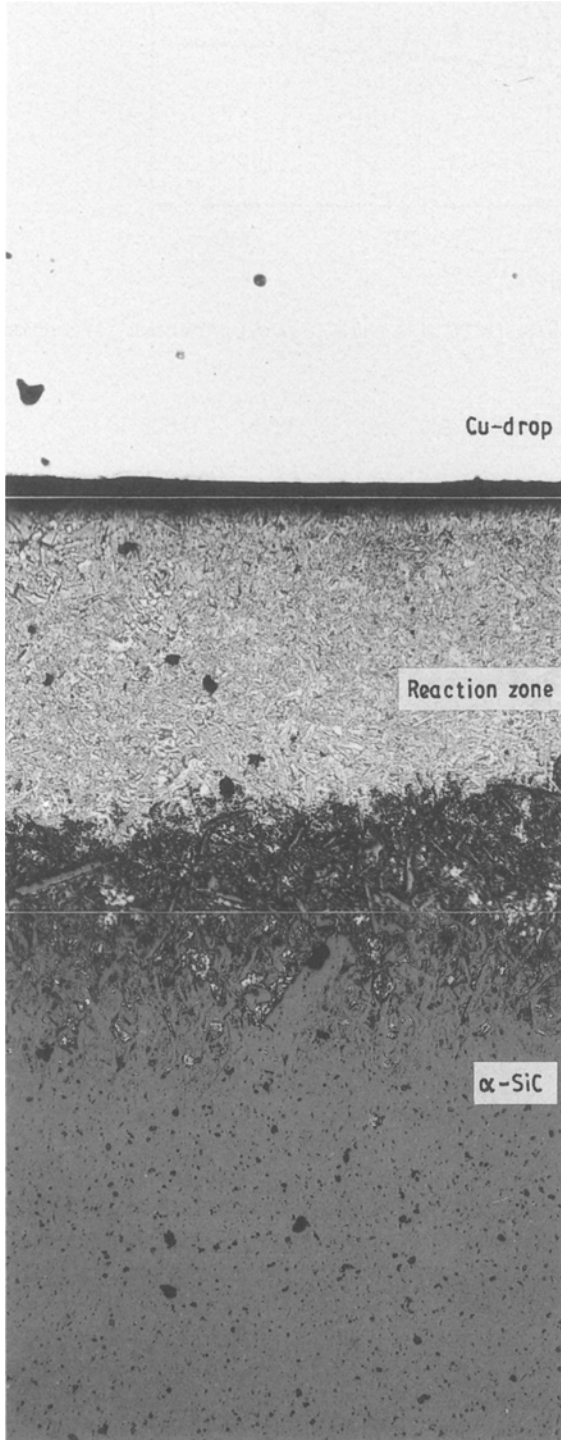


Figure 8 Reaction zone between Cu and  $\alpha$ -SiC ( $T = 1583$  K,  $t = 20$  min in argon).

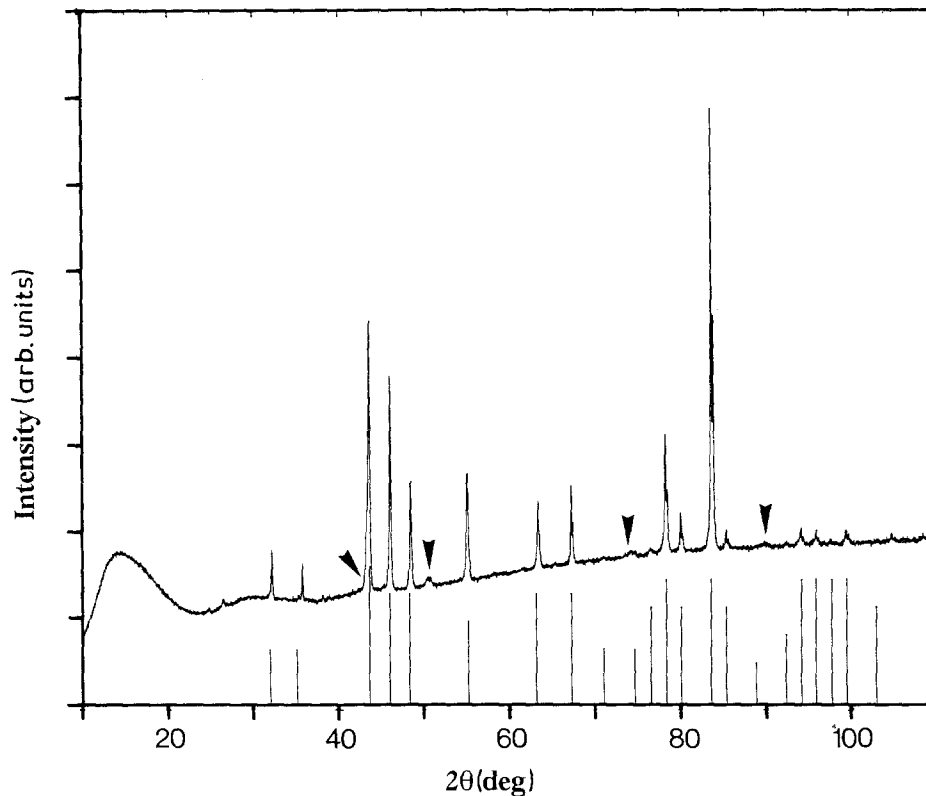


Figure 9 XRD patterns of the copper melt and the reaction zone with  $\alpha$ -SiC at 1873 K (4 h).  $\text{Cu}_5\text{Si}$  ( $\gamma$ -phase); arrowheads, Cu ( $\alpha$ -phase).

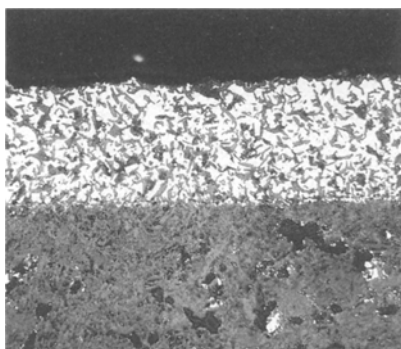


Figure 10 Cross-section of  $\beta$ -SiC layer after the reaction with Ni.

at 1770 K. He observed the dihedral angle  $\psi < 60^\circ$  for a pore at the grain boundary in SiC.

#### 4. Conclusions

The contact angle  $\theta$  formed between different SiC qualities and molten Si and the metals Sn, Cu, Ni has been determined experimentally.

1. At temperatures near its melting point silicon wets all investigated SiC qualities and the contact angle is independent of time. For mono- as well as polycrystalline  $\alpha$ -SiC,  $\theta \approx 38^\circ$  and for  $\beta$ -SiC,  $\theta \approx 41.5^\circ$ .

2. Tin does not wet the SiC. The temperature dependence of the work of adhesion and of the interfacial energy can be given as follows:

$$W_\alpha(\alpha\text{-SiC-Sn}) = 0.047 + 0.192 \times 10^{-3} (T - 505) \text{ (Jm}^{-2}\text{)}$$

$$\gamma_{\text{SL}}(\alpha\text{-SiC-Sn}) = 3.629 - 0.808 \times 10^{-3} (T - 505) \text{ (Jm}^{-2}\text{)}$$

3. Copper and nickel react with silicon carbide. The silicon content of the copper drop depends on the temperature and after solidification consists of the  $\alpha$ -Cu or  $\gamma$ -Cu phase. After cooling, the nickel drop forms the compound  $\text{Ni}_3\text{Si}_2$ .

4. Successful thermal etching of polycrystalline  $\alpha$ -SiC at 2020 K in vacuum allows the determination of groove angle  $\theta$  as  $157.6 \pm 5.8^\circ$ . Therefore  $\gamma_{\text{SS}}$  was estimated to be  $0.733 \text{ Jm}^{-2}$ .

#### Acknowledgements

The present work was performed within the framework of bilateral Greek-German cooperation between the Ministries of Research and Technology of Greece and Germany. The authors appreciate the technical assistance given by Mr A. Schirbach.

#### References

1. G. ZIEGLER, "Keramische Konstruktionswerkstoffe-Stand der Technik" (VDI-Tagung, Essen, April 1987) p. 1.
2. G. WILLMANN, *Keram. Z.* **36** (1984) 669.
3. P. NIKOLOPOULOS, G. ONDRACEK and D. SOTIROPOULOU, *Ceram. Int.* **15** (1989) 201.
4. S. AMELINCKX, N. F. BINNEDIJK and W. DEKEYSER, *Physica* **19** (1953) 1173.
5. F. BASHFORT and S. C. ADAMS, "An Attempt to Test the Theories of Capillary Action" (Cambridge University Press, Cambridge, 1983).
6. T. J. WHALEN and A. T. ANDERSON, *J. Amer. Ceram. Soc.* **58** (1975) 396.
7. Yu. V. NAIDICH and G. M. NEVODNIK, *Bull. Acad. Sci. USSR - Inorg. Mater.* **5** (1969) 2066.

8. V. L. YUPKO and G. G. GNESIN, *Poroshka. Met.* **130** (1973) 97.
9. W. KÖHLER, *Aluminium* **51** (1975) 443.
10. B. C. ALLEN and W. D. KINGERY, *Trans. Met. Soc. AIME* **215** (1959) 30.
11. P. NIKOLOPOULOS and G. ONDRACEK, "Verbundwerkstoffe" (Deutsche Gesellschaft für Metallkunde (DGM), Oberursel, 1981) p. 391.
12. M. HANSEN and K. ANDERKO, "Constitution of Binary Alloys" (McGraw-Hill, New York, 1958).
13. G. G. GNESIN and Yu. V. NAIDICH, *Poroshka Met.* **2** (1969) 57.
14. J. T. KLUMP, in "Designing Interfaces for Technological Applications", edited by S. D. Peteves (Elsevier, London, 1989) p. 127.
15. M. R. JACKSON, R. L. MEHAN, A. M. DAVIS and E. L. HALL, *Metall. Trans. A.* **14A** (1983) 355.
16. R. H. BRUCE, in "Science of Ceramics", Vol. 2, edited by G. H. Stewart (Academic, London, 1965) p. 359.
17. B. C. ALLEN, in "Liquid Metals", edited by S. Z. Beer (Dekker, New York, 1972) p. 161.
18. G. LANG, *Z. Metallkde* **67** (1976) 549.
19. W. P. MINNEAR, *J. Amer. Ceram. Soc.* **65** (1982) C10.
20. R. WARREN and C.-H. ANDERSSON, *Composities* **15** (1984) 101.

*Received 11 September 1990  
and accepted 28 February 1991*